Published in final edited form as:

Anal Chem. 2018 September 18; 90(18): 11062–11069. doi:10.1021/acs.analchem.8b02907.

Online Liquid Chromatography - Sheath-Flow Surface Enhanced Raman Detection of Phosphorylated Carbohydrates

Anh H. Nguyen[a], **Jessica M. Deutsch**[a], **Lifu Xiao**[b], and **Zachary D. Schultz**[*,a,b]

[a] Department of Chemistry and Biochemistry, University of Notre Dame, Notre Dame, IN 46556, United States

[b] Department of Chemistry and Biochemistry, The Ohio State University, Columbus, OH 43210, United States

Abstract

Online detection and quantification of three phosphorylated carbohydrate molecules: glucose 1-phosphate, glucose 6-phosphate and fructose 6-phosphate was achieved by coupling sheath-flow surface enhanced Raman spectroscopy (SERS) to liquid chromatography. The presence of an alkanethiol (hexanethiol) self-assembled monolayer adsorbed to a silver SERS-active substrate helps retain and concentrate the analytes of interest at the SERS substrate to improve the detection sensitivity significantly. Mixtures of 2 μM of phosphorylated carbohydrates in pure water as well as in cell culture media were successfully separated by HPLC, with identification using the sheath-flow SERS detector. The quantification of each analyte was achieved using partial least squares (PLS) regression analysis and acetonitrile in the mobile phases as an internal standard. These results illustrate the utility of sheath-flow SERS for molecular specific detection in complex biological samples appropriate for metabolomics and other applications.

Graphical abstract

Authors are required to submit a graphic entry for the Table of Contents (TOC) that, in conjunction with the manuscript title, should give the reader a representative idea of one of the following: A key structure, reaction, equation, concept, or theorem, etc., that is discussed in the manuscript. Consult the journal's Instructions for Authors for TOC graphic specifications.

[*]**Corresponding Author:** Schultz.133@osu.edu.

Author Contributions

The manuscript was written through contributions of all authors. All authors have given approval to the final version of the manuscript.

DISCLOSURE

The corresponding author is an inventor on the sheath-flow SERS flow cell. The patent is currently not licensed.

ASSOCIATED CONTENT

Supporting Information

The Supporting Information is available free of charge on the ACS Publications website at DOI:

Spontaneous Raman spectra of 0.5 M solutions of glucose 1phosphate, glucose 6-phosphate and fructose 6-phosphate; SERS spectra of glucose 1-phosphate, glucose 6-phosphate and fructose 6-phosphate obtained on bare silver SERS-active substrate and 4mercaptophenylboronic acid (4-MPBA) SAM silver substrate; table of SERS peaks assignments for each analyte; details of PLS regression analysis for calibration model and cross-validation from experimental samples. (PDF)

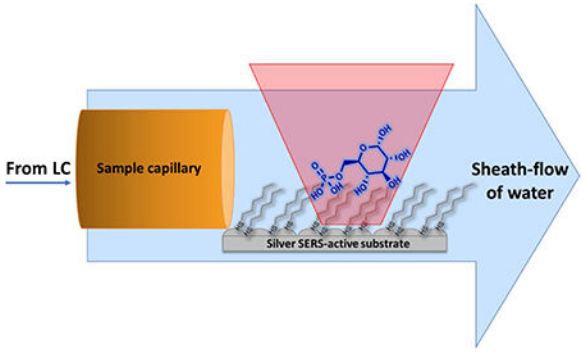

INTRODUCTION

Metabolomics has risen to prominence recently with the advent of technologies that enable the rapid identification of biomolecules found in biological fluids.[1] The tremendous amount of previous knowledge about biochemical pathways enables a systems biology approach to interpreting changes in the levels of detected metabolites. There are over 40,000 entries in the Human Metabolome Database, the most complete record of known metabolites;[2] however, most metabolomics studies can only confirm the identity of a small fraction of the metabolites in a sample. The ability to monitor the levels of multiple specific metabolites and analyze changes is key to identifying misregulated pathways associated with disease. Currently, the leading technologies available for metabolomics largely consist of nuclear magnetic resonance (NMR) and mass spectrometry (MS).[3–6]

Phosphorylated carbohydrates are key intermediates in biochemical pathways.[7–8] The differential phosphorylation of glucose is associated with different biological processes. The conversion of glucose to glucose 6-phosphate (G6P) by hexokinases, and G6P to fructose 6-phosphate (F6P) by G6P isomerase are known steps in glucose metabolism pathways. Phosphorylation is a key modification that prevents the secretion of glucose out of the cell by glucose transporters. G6P also serves as a central point for both glycolysis and glycogenesis, in which the G6P is converted into glucose 1-phosphate (G1P) to produce glycogen. G6P is also the starting metabolite in the pentose phosphate pathway.[9] Targeted metabolomics of phosphorylated carbohydrates, especially the glycolytic intermediates, is key to monitoring changes in metabolism associated with diseases, such as cancer.[7, 10] However, quantitative analysis of phosphorylated sugars remains challenging due to difficulties in the chromatographic separation, where the isomers often coelute or have very close retention times. Additionally, these molecules lack specific fragmentation patterns in mass spectrometry, and multiple isomers show similar mass to charge ratios.[11–12]

The current mass spectrometry approach to solve this problem is to use ion trap and ion mobility spectrometry to provide sequential mass spectrometry (MS^n) and separations based on the analyte ions' size, shape and their mobility rather than their mass.[13–14] This approach is time consuming, and it has been reported that MS^2 or MS^3 will not decipher all isomers and requires multiple stages of MS for full characterization.[14]

Recent developments in surface enhanced Raman scattering (SERS) suggests a straight forward method to characterizing phosphorylated carbohydrates and other isomeric metabolites.[15] Because the Raman spectrum is sensitive to the structure of the molecule, isomers can be readily distinguished. The increased sensitivity associated with SERS detection, relative to spontaneous Raman, makes it an attractive analytical technique. To improve throughput in SERS analysis, recent reports have shown methods for direct coupling with HPLC separations.[16–18] Most LC-SERS approaches introduce colloids and aggregating agents into the mobile phase following the separation to enable at-line SERS detection. Previous work in our lab demonstrated that hydrodynamic focusing onto a planar substrate provides increased sensitivity SERS detection in flowing solutions,[19] and is readily incorporated for online detection following a chemical separation.[20] This sheath-flow SERS detection has been demonstrated for capillary electrophoresis, and more recently, capillary-LC separations.[18, 21]

Here we demonstrate the use sheath-flow with LC-SERS detection to identify and quantify three different phosphorylated carbohydrates: glucose 6-phosphate (G6P), glucose 1-phosphate (G1P) and fructose 6-phosphate (F6P). The increased sensitivity and chemical specificity of SERS is used to differentiate the phosphorylated sugars. To improve the selectivity and sensitivity for phosphorylated carbohydrates, a hydrophobic monolayer is formed on the SERS substrate. By coupling sheath-flow SERS with a LC separation, these structural isomers can be characterized in a complex biological environment. Therefore, coupling sheath-flow SERS online with LC presents an interesting approach for rapid nondestructive detection of metabolites that can be run orthogonal to other standard analysis, such as LC-MS, ion mobility spectrometry or NMR, to characterize isomeric analytes.

EXPERIMENTAL SECTION

Material and Reagents

α-D-Glucose 1-phosphate disodium salt hydrate (≥97%), DGlucose 6-phosphate disodium salt hydrate (≥98%), DFructose 6-phosphate disodium salt hydrate (≥98%), acetonitrile (HPLC graded), ammonium hydroxide (HPLC graded) were purchased from Sigma-Aldrich (St. Louis, MO). Dulbecco’s Modified Eagle Medium (DMEM) media with no glucose, glutamine or phenol red added was used without further purification. Nanopure water (18.2 MΩ cm) was obtained from a Barnstead Nanopure filtration system. Bare fused silica capillary with 41.5 μm i.d. and 104 μm o.d. was purchased from Polymicro Technologies (Phoenix, AZ).

SERS substrate preparation

The SERS-active substrate was prepared by a thermal evaporation protocol as previously reported.[22] In this report the procedure was slightly modified to enable the addition of an alkane-thiol monolayer. Briefly, silver shot was evaporated onto an aluminum anodized oxide (AAO) filter with 0.1 μm pores. The substrate was then soaked in 10 mM ethanolic solution of hexanethiol for 24 hours to form a monolayer. The AAO filter was then removed by submerging in 0.1 M sodium hydroxide solution for 4 hours, leaving behind a thin layer

of hexanethiol SAMs on the silver substrate. Prior to the experiment, the substrate was affixed on a glass slide and incorporated into a custom-built SERS flow cell.

Sample preparation

All solutions of G1P, G6P and F6P were prepared in 50/50 (v/v) of water/acetonitrile (0.1% NH_4OH). A series of standard solutions were prepared for each analyte ranging from 0.25 μM to 20 μM for standard SERS calibration tests. For LCSERS experiments, mixtures of each analyte were prepared in 50/50 (v/v) of water/acetonitrile (0.1% NH_4OH) or a 10x dilution of no glucose DMEM cell media prior to injections.

Liquid Chromatography

Chromatographic separation was achieved using a capillary Ultimate LC Packings system with quaternary pumps and a 1 μL injection loop. Separations and chromatograms were controlled and obtained by Ultichrom software (LC Packings). An amide column (Inertsil, 50 × 0.3 mm, 3 μm), which is known for its ability to retain extremely polar compounds, was used in this experiment. Mobile phase A consisted of 80/20 acetonitrile/water (0.1% NH_4OH) and mobile phase B consisted of 30/70 acetonitrile/water (0.1% NH_4OH) were pumped at 2 μL/min with gradient from 100% A to 60% A in 10 minutes. After each run, the column was reconditioned with 95% A for 15 minutes.

Raman detection

Raman spectroscopy was performed using a homebuilt setup as previously described.[23] In general, a 17 mW (cw), 632.8 nm HeNe laser was focused onto the SERS-active substrate in the flow cell through a 40x water immersion objective (Olympus, NA=0.8). Raman scattering was collected through the same objective and directed to the Shamrock 303i spectrograph (Andor) and EMCCD (Newton 970, Andor). Raman spectra were recorded in series with a 100 ms acquisition time and 1.5 mW of laser power at the sample.

LC-SERS

The instrumental setup for online post-column chromatographic SERS detection has been previously described.[18] A 22 cm long fused silica was used to connect the LC outlet to the customized SERS flow cell[19] through a PEEK union. The end of the capillary was affixed in the center of the SERS substrate. Analyte confinement on SERS substrate was achieved by hydrodynamic focusing by pumping a sheath fluid (water) at 140 μL/min through the sample inlet and outlet on the flow cell while keeping the analyte flow rate out of the sample capillary at 2 μL/min.

Data analysis

All SERS spectra and LC chromatograms were processed by Matlab 2015a (Mathworks). SERS spectra row normalization and partial least square (PLS) regression analysis were performed by the PLS toolbox (Eigenvector Research, Inc.) operating in Matlab.

RESULT

To identify the SERS spectrum of the phosphorylated carbohydrates, reference spectra were acquired using sheath-flow SERS detection. Figure 1 shows the SERS spectra obtained from G1P, G6P and F6P at different concentrations using the sheath-flow SERS cell. In these experiments, improved signal was obtained by functionalizing the SERS substrate with a hexanethiol monolayer. The hexanethiol monolayer provides a constant background (Figure 1d), which was subtracted from the Raman signals observed from each of the analytes.

The analyte spectra were obtained by direct injection, where the analytes were prepared at the concentrations indicated in the mobile phase to be used in LC-SERS experiments. A 1 μL sample was injected into the SERS-flow cell using the LC pump without the column. The phosphate stretching mode at ~921 cm^{-1} was observed in SERS spectrum of all three analytes. Other common peaks between three analytes include peaks at 1070 cm^{-1} (C-OH stretching), 1120 cm^{-1} (C-C/C-O stretching) and 1345 cm^{-1} (C-C-H bending), which correspond with the previously reported SERS signals of glucose.[24–26] Tentative peaks assignment for each analyte are reported in Table S-1. The observed spectra show similar frequencies to the spontaneous Raman spectrum of each analyte (Figure S-1). The CN stretch of acetonitrile was observed at 2250 cm^{-1} and treated as an internal standard for quantitative analysis, as previously reported.[18] The SERS intensities in Figure 1 have been backgournd subtracted to remove the signal from the alkanethiol monolayer and row normalized, as shown in Figure 1d. Alkanethiols are expected to form a monolayer coverage and give rise to a consistent SERS background due to the bond between the sulfur and Ag. SERS peaks observed from the hexanethiol monolayer are at 712 cm^{-1} (C-S stretch), 868 (CH_2 rock), 897 cm^{-1} (CH_3 rock), 1013 cm^{-1} (CH_3 rock), 1032 cm^{-1} (C-C stretch), 1122 cm^{-1} (C-C stretch), 1337 cm^{-1} (CH_2 wag) and 1445 cm^{-1} (CH_2 deformation).[24, 26–27]

The presence of the alkanethiol monolayer greatly increased the sensitivity of the SERS experiments. Figure S-2 shows the SERS spectra of G1P and G6P at 250 μM on bare silver substrate obtained at 2 mW laser power and 250 ms acquisition time. Attempts to obtain G1P, G6P and F6P SERS signals on bare silver substrate at low concentrations were largely unsuccessful and lacked reproducibility. On bare silver, the spectra show very poor signal to noise ratios. Previous work has shown that SERS detection in solution is dependent on adsorption of the analyte to the SERS substrate.[22] Glucose, however, is reported to have a low affinity for metal.[24, 28]

Previous work with SERS based glucose sensors has shown that alkyl-monolayers improve the SERS response by confining glucose molecules closer to the SERS-active substrate.[24–25,29] The analyte-SAM interactions can retain and concentrate the analytes of interest at the monolayer interface for detection. For example, mercapto-phenylboronic acid functionalized monolayers have been used in SERS-based glucose sensors due to the selective binding between the boronic acid and the cis-diols on glucose, forming a cyclic boronate ester linkage.[28,30] The process is rapid in basic solution and reversible by reconditioning the substrate in acidic solution. While this approach works well for glucose, our experiments to detect phosphorylated carbohydrates using 4-mercaptophenylboronic acid SAM on silver substrates were unsuccessful. At the basic pH where the cyclic boronate

linkage forms, the phosphate is also negatively charged. Charge repulsion appears to occur between the boronic acid group and the phosphate group on the analyte under our experimental conditions preventing detection (see Figure S-3). Instead of relying on analyte-SAM chemical binding, an unfunctionalized alkyl monolayer can provide increased adsorption and retention of analytes of interest, similar to the column stationary phase in chromatographic experiments. In our study, hexanethiol was used to form a monolayer on top of the SERS-active substrate to improve the detection of phosphorylated carbohydrates molecules.

A mixture containing 2 μM of G1P, G6P and F6P were used to assess the quantitative separation and detection of the analytes by LC-SERS. Figure 2a shows the LC-SERS separation of the phosphorylated carbohydrates. The sheath-flow SERS cell was connected in series with a commercial LC system for SERS detection as previously described.[18]

Figure 2a shows the 3D heat map of SERS intensity as a function of Raman shift and retention time following an LC separation. The SERS heatmap indicates that F6P, G1P, and G6P eluted onto the substrate at 2.6 ± 0.3 mins, 3.0 ± 0.3 mins and 3.5 ± 0.2 mins respectively. The observed retention peaks show the same narrowing that has been previously observed in capillary-electrophoresis separations with sheath flow SERS detection.[21] Similar to these previous results, the retention width is narrowed in a fashion proportional to concentration such that only the highest concentration portion of the elution peak is detected. Although the retention times are very close, sheath-flow SERS is able to resolve the individual molecules due to the narrower elution peak-widths and short signal durations compared to other types of detectors. An advantage of SERS detection is the ability to detect and characterize analytes, such as these phosphorylated sugars, that do not absorb light in the wavelength range common of UV-Vis detectors incorporated with HPLC or that are below the UV-Vis limit of detection. To confirm the analyte identification, Figure 2b shows the extracted SERS spectrum of each analyte from the separation compared with the reference spectra determined from the direct injection experiments in Figure 1. The agreement with the reference SERS spectrum validates the identification.

To assess our ability to quantify the phosphorylated carbohydrates, Figure 3a-c shows the PLS regression models, established from the concentration dependent spectra in Figure 1, plotting the predicted concentrations versus the measured concentrations. Challenges associated with quantitative SERS studies are well known and have been attributed to day-to-day substrate variation, drift in laser power or competitive adsorption between analytes to the SERS-active substrate. It is worth pointing out that a single SERS substrate can be used for a few separations, which required multiple different substrates to acquire the calibration and validation data. An internal standard is key to comparing across different substrates. In our previous LC-SERS work[18], we demonstrated that acetonitrile in the mobile phase can serve as an internal standard for quantitative SERS detection. Again, we have employed acetonitrile as an internal standard for improved quantification.

The spectra of G1P, G6P and F6P at different concentrations ranging from 0.25 μM to 20 μM (Figure 1a-c) were normalized against the intensity of acetonitrile at 2250 cm^{-1} before being employed to construct calibration models using partial least square (PLS) regression

analysis as shown in Figure 3a-c. Each data point is an average of the SERS spectra taken during the direct injection process, representing approximately 200 spectra in total. Four or five replicates were obtained for each concentration. A PLS regression model was built to analyze the full spectra and yield a more accurate result based on the relationship between concentration and SERS signal intensities. Row normalization and mean centering were carried out prior to constructing the PLS model. The number of latent variables were optimized using PLS toolbox to minimize the root mean square of cross-validation values. Details of PLS regression analysis are shown in SI. The minimum root mean square error of cross-validation of all three analytes were found to be 2.75 μM for G1P, 0.90 μM for G6P, 1.71 μM for F6P. The root mean square errors of calibration for each calibration set were also determined to be 1.92 μM, 0.72 μM, and 0.88 μM for G1P, G6P and F6P, respectively. The inset plots in Figure 3a-c show PLS calibration model built on SERS spectra of each analyte without the internal standard. As expected, the plots are not linear and show larger variance without the internal standard.

Using the calibration model established in Figure 3, the known analyte concentrations from the mixture were then correlated back to the calibration model (red data points) to test the reliability of the PLS regression analysis. Based on our result, the validation data and the loading model are in good square errors of predictions were calculated to be 0.84 μM, 1.20μM, and 0.30 μM for G1P, G6P and F6P, respectively. Physiological concentrations of phosphorylated carbohydrates are reported to range from 10 – 30 μM in biological samples, [31] which suggests our model can be applied to detect and quantify these analytes in a biological environment.

To test the capabilities in a biological matrix, the phosphorylated carbohydrates were spiked into glucose free cell culture media. Figure 4a shows LC-SERS chromatogram of the complex mixture plotted as Raman shift on the y-axis and time on the x-axis. Multiple signals are recorded in the SERS flow detector from various components of the cell culture media. Several molecules closely elute onto the substrate with similar retention times to the analytes of interest between 2.5 – 4 mins, which creates challenges to isolate the SERS spectra of the analytes. Therefore, to identify the observed spectra of the analytes from other species in the sample, we used a Pearson's correlation to comparare against the reference spectrum of each analyte. This approach was previously used to successfully identify bezoylecgonine spiked into urine and separated by capillary electrophoresis.[32] The Pearson correlation coefficient was calculated between every spectrum in the LC-SERS run against the reference spectra for F6P, G1P, and G6P independently, as shown in Figure 4b. The Pearson's correlation coefficient determines the degree of linear correlation (dependence) between two spectra on a scale from −1 to 1 where 1 is total positive correlation, 0 is no correlation and −1 is negative correlation. The highest correlation for each analyte was observed in the complex separation at a retention time comparable to the simple mixture in Figure 2a. The SERS spectra at the time points corresponding to the highest correlation were extracted and compared to the reference spectra to further confirm the identification of the analytes. Figure 5a-c shows how the SERS spectra of G1P, G6P and F6P compare to their reference spectra, respectively. The frequencies observed in Figure 5 are in excellent agreement with the reference spectra for the appropriate analyte. Some minor differences in peak intensity are observed, which are common in SERS experiments. [33]

The concentration of the analytes spiked into the cell culture media were determined using the internal standard and PLS regression model applied in Figure 3. Figure 6 shows how the SERS signals from the phosphorylated carbohydrates in cell culture media (red data points) correspond to the calibration model. The results are in good agreement with the calibration data for all three analytes, as the test data points project along the red fit line. By obtaining a clean spectrum, a calibration model established from simple components can be used to quantify analytes in complex samples. Root mean square errors of predictions were calculated to be 2.48 μM, 1.78 μM, and 1.95 μM for G1P, G6P and F6P respectively. The errors of predictions are slightly greater in the cell media data set compared to the case of the simple mixture. The increased error of prediction is not entirely unexpected. The SERS detection is sensitive to the compounds that interact with the surface. When multiple compounds are present in complex samples, they can compete for surface sites. The observed SERS spectrum will be weighted by the most abundant species, consistent with our identification at specific retention times. However, other species that displace the acetonitrile molecules, without evincing significant Raman scattering, will affect the calibration. This suggests that quantitative detection is still dependent upon high quality separations to avoid interference, such as was demonstrated in the simple mixture.

DISCUSSION

Our results show that sheath-flow SERS is capable of online detection and quantitative analysis of phosphorylated carbohydrate isomers following a capillary liquid chromatography separation. Our results illustrate new possibilities for sensing using SERS coupled to liquid chromatography separations.

The enhancement of SERS signals relies strongly on the proximity of the molecules to the nanostructures surface exhibiting strong local surface plasmon resonance. Well regarded theories of SERS report that the enhancement decays with distance from the surface.[34] In our study, the limit of detection was improved by the addition of a short (hexanethiol) alkyl monolayer on the SERS substrate. This monolayer prevents analytes from direct interaction with the metal nanostructure; however, the monolayers changes the surface chemistry and can promote adsorption of the analytes. The importance of adsorption for SERS detection is consistent with previous results obtained from particles in solution.[22] Adsorption has also been implicated in sensitive SERS studies by others, for example the Kamat group reported constructing silver particles on graphene improved detection through adsorption to the graphene.[35] Our result indicates that chemical modification to alter surface chemistry and promote adsorption is a general approach to increasing detection sensitivity of different classes of analytes.

The formation of alkanethiols monolayer over the surface of SERS silver substrate is advantageous for partitioning the phosphorylated carbohydrate molecules, providing improved SERS detection. Addition of the monolayer overcomes many challenges previously reported for SERS detection of these molecules.[26, 28–29] The SERS adsorption problems of the analytes have been resolved by concentrating the analytes in the hydrophobic monolayer and within the ‘hotspot’ of electromagnetic field enhancement. As the concentration of the analyte in the mobile phase decreases, the analyte desorbs. This

reversible interaction enables online detection following chromatographic separations. Moreover, the SAM-analyte interactions provide an interesting approach to obtain direct SERS signals of biomolecules that have weak adsorption to metal substrate. Additionally, one end of the alkane chain monolayer can be modified with a terminal functional group, such as an amine, to capture a different range of biofunctional moieties at the surface.[36] Carboxylic acids (COOH) are another terminal group that has the ability to bind to amines that are present in proteins, peptides or oligonucleotides such as DNA or RNA.[37] The alkanethiol monolayer also protects the silver substrate from being oxidized so it can stay stable throughout multiple runs.

Only a few reports have shown the combination of LC and SERS for online separation and detection.[16–18, 38–39] These reports commonly rely on mixing the LC eluent with aggregated nanoparticles.[39–40] Recently, the Goodacre group reported that introducing an aggregation agent with silver colloids following separation allows for quantitative analysis of drugs and drug metabolites.[38] Approaches using colloids utilize significant resources to add nanoparticles to each fraction, or require prior optimization of the separation to identify the relevant elution fractions for SERS analysis. Additionally, postcolumn conditions, such as changes in pH, can affect the nanoparticle aggregation process and resulting SERS response. Lendl and co-workers were able to optimize pH conditions in the individual wells of a multi-well plate for efficient SERS detection, but they noted the separation needed to be optimized first.[16] The LC - sheath-flow SERS facilitates online, high-throughput detection of analytes. Additionally, a hydrophobic layer can be readily incorporated with an aqueous, reverse phase separation. The SERS cell is connected directly to the LC outlet, creating a closed flow path that allows real time detection of the molecules. The molecules are not contaminated with additional reagents, which may enable further downstream analysis. Optimization of the sheath-flow cell design can minimize the dilution of analytes by the sheath flow to preserve the sample.[23]

In addition to phosphorylated carbohydrates, in-flow LCSERS provides a chemically specific method for the detection of other closely related biomolecules, such as isomer and protein isoforms. Previous SERS studies have successfully detected single base mismatch in nucleic acids sequences and DNA modifications.[41] SERS has also detected and quantified entacapone E and Z isomers, an inhibitor for Parkinson's disease.[42] The sensitivity to subtle molecular changes in the presence of complex Raman signals from biological environment suggests sheath-flow SERS provides an interesting approach for identifying biomolecules in separations relevant to many biological conditions.

CONCLUSION

We demonstrate that chemical modification of planar SERS substrate combined with sheath-flow SERS enables online identification and quantification of glucose-1-phosphate, glucose-6-phosphate, and fructose-6-phosphate in a complex biological matrix. The addition of the alkyl-monolayer enabled detection of these compounds at ~1 μM concentrations, well below concentrations typically observed in cells. The linear dynamic range extends through the biologically relevant range of 10–20 μM. Furthermore, the addition of the alkyl monolayer alters the surface chemistry to promote interactions between the analytes and the

SERS substrate, and suggests a general strategy for controlling the selectivity of online LCSERS detection.

Supplementary Material

Refer to Web version on PubMed Central for supplementary material.

ACKNOWLEDGMENT

This work was supported by the National Science Foundation Award DBI-1455445 and the National Institutes of Health, Nattional Cancer Institute Award R33 CA206922.

REFERENCES

1. Patti GJ; Yanes O; Siuzdak G, Innovation: Metabolomics: the apogee of the omics trilogy. Nat Rev Mol Cell Biol 2012, 13 (4), 263–9. [PubMed: 22436749]
2. Wishart DS; Jewison T; Guo AC; Wilson M; Knox C; Liu Y; Djoumbou Y; Mandal R; Aziat F; Dong E; Bouatra S; Sinelnikov I; Arndt D; Xia J; Liu P; Yallou F; Bjorndahl T; Perez-Pineiro R; Eisner R; Allen F; Neveu V; Greiner R; Scalbert A, HMDB 3.0--The Human Metabolome Database in 2013 Nucleic Acids Res 2013, 41 (Database issue), D801–7.
3. Theodoridis G; Gika HG; Wilson ID, LC-MS-based methodology for global metabolite profiling in metabonomics/metabolomics. Trac-Trends Anal. Chem. 2008, 27 (3), 251–260.
4. Beckonert O; Keun HC; Ebbels TMD; Bundy J; Holmes E; Lindon JC; Nicholson JK, Metabolic profiling, metabolomic and metabonomic procedures for NMR spectroscopy of urine, plasma, serum and tissue extracts. Nat. Protocols 2007, 2 (11), 2692–2703. [PubMed: 18007604]
5. Johnson CH; Gonzalez FJ, Challenges and opportunities of metabolomics. J Cell Physiol 2012, 227 (8), 2975–81. [PubMed: 22034100]
6. Suhre K, Metabolic profiling in diabetes. Journal of Endocrinology 2014, 221 (3), R75–R85. [PubMed: 24868111]
7. Lucarelli G; Galleggiante V; Rutigliano M; Sanguedolce F; Cagiano S; Bufo P; Lastilla G; Maiorano E; Ribatti D; Giglio A; Serino G; Vavallo A; Bettocchi C; Selvaggi FP; Battaglia M; Ditonno P, Metabolomic profile of glycolysis and the pentose phosphate pathway identifies the central role of glucose-6phosphate dehydrogenase in clear cell-renal cell carcinoma. Oncotarget 2015, 6 (15), 13371–86. [PubMed: 25945836]
8. Weckmann K; Diefenthaler P; Baeken MW; Yusifli K; Turck CW; Asara JM; Behl C; Hajieva P, Metabolomics profiling reveals differential adaptation of major energy metabolism pathways associated with autophagy upon oxygen and glucose reduction. Sci Rep 2018, 8 (1), 2337. [PubMed: 29402948]
9. Peoples JNR; Maxmillian T; Le Q; Nadtochiy SM; Brookes PS; Porter GA, Jr.; Davidson VL; Ebert SN, Metabolomics reveals critical adrenergic regulatory checkpoints in glycolysis and pentose-phosphate pathways in embryonic heart. J Biol Chem 2018, 293 (18), 6925–6941. [PubMed: 29540484]
10. Williams MD; Zhang X; Park JJ; Siems WF; Gang DR; Resar LM; Reeves R; Hill HH, Jr., Characterizing metabolic changes in human colorectal cancer. Anal Bioanal Chem 2015, 407 (16), 4581–95. [PubMed: 25943258]
11. Ross KL; Dalluge JJ, Liquid chromatography/tandem mass spectrometry of glycolytic intermediates: deconvolution of coeluting structural isomers based on unique product ion ratios. Anal Chem 2009, 81 (10), 4021–6. [PubMed: 19354282]
12. Kailemia MJ; Ruhaak LR; Lebrilla CB; Amster IJ, Oligosaccharide analysis by mass spectrometry: a review of recent developments. Anal Chem 2014, 86 (1), 196–212. [PubMed: 24313268]
13. Lanucara F; Holman SW; Gray CJ; Eyers CE, The power of ion mobility-mass spectrometry for structural characterization and the study of conformational dynamics. Nat Chem 2014, 6 (4), 281–94. [PubMed: 24651194]

14. Ashline DJ; Lapadula AJ; Liu YH; Lin M; Grace M; Pramanik B; Reinhold VN, Carbohydrate structural isomers analyzed by sequential mass spectrometry. Anal Chem 2007, 79 (10), 3830–42. [PubMed: 17397137]
15. Nguyen AH; Peters EA; Schultz ZD, Bioanalytical applications of surface-enhanced Raman spectroscopy: de novo molecular identification. In Reviews in Analytical Chemistry, 2017; Vol. 0.
16. Carrillo-Carrion C; Armenta S; Simonet BM; Valcarcel M; Lendl B, Determination of pyrimidine and purine bases by reversed-phase capillary liquid chromatography with at-line surfaceenhanced Raman spectroscopic detection employing a novel SERS substrate based on ZnS/CdSe silver-quantum dots. Anal Chem 2011, 83 (24), 9391–8. [PubMed: 22047639]
17. Cowcher DP; Jarvis R; Goodacre R, Quantitative online liquid chromatography-surface-enhanced Raman scattering of purine bases. Anal Chem 2014, 86 (19), 9977–84. [PubMed: 25196415]
18. Nguyen A; Schultz ZD, Quantitative online sheath-flow surface enhanced Raman spectroscopy detection for liquid chromatography. Analyst 2016, 141 (12), 3630–5. [PubMed: 27067384]
19. Negri P; Jacobs KT; Dada OO; Schultz ZD, Ultrasensitive surface-enhanced Raman scattering flow detector using hydrodynamic focusing. Anal Chem 2013, 85 (21), 10159–66. [PubMed: 24074461]
20. Negri P; Flaherty RJ; Dada OO; Schultz ZD, Ultrasensitive online SERS detection of structural isomers separated by capillary zone electrophoresis. Chem Commun (Camb) 2014, 50 (21), 2707–10. [PubMed: 24395125]
21. Asiala SM; Schultz ZD, Surface enhanced Raman correlation spectroscopy of particles in solution. Anal Chem 2014, 86 (5), 2625–32. [PubMed: 24502388]
22. Bailey MR; Pentecost AM; Selimovic A; Martin RS; Schultz ZD, Sheath-flow microfluidic approach for combined surface enhanced Raman scattering and electrochemical detection. Anal Chem 2015, 87 (8), 4347–55. [PubMed: 25815795]
23. Shafer-Peltier KE; Haynes CL; Glucksberg MR; Van Duyne RP, Toward a Glucose Biosensor Based on SurfaceEnhanced Raman Scattering. Journal of the American Chemical Society 2003, 125 (2), 588–593. [PubMed: 12517176]
24. Yonzon CR; Haynes CL; Zhang X; Walsh JT; Van Duyne RP, A Glucose Biosensor Based on Surface-Enhanced Raman Scattering: Improved Partition Layer, Temporal Stability, Reversibility, and Resistance to Serum Protein Interference. Analytical Chemistry 2004, 76 (1), 78–85. [PubMed: 14697035]
25. Rycenga M; McLellan JM; Xia Y, A SERS study of the molecular structure of alkanethiol monolayers on Ag nanocubes in the presence of aqueous glucose. Chemical physics letters 2009, 463 (1–3), 166–171. [PubMed: 20160847]
26. Bryant MA; Pemberton JE, Surface Raman scattering of self-assembled monolayers formed from 1-alkanethiols: behavior of films at gold and comparison to films at silver. Journal of the American Chemical Society 1991, 113 (22), 8284–8293.
27. Kong KV; Ho CJH; Gong T; Lau WKO; Olivo M, Sensitive SERS glucose sensing in biological media using alkyne functionalized boronic acid on planar substrates. Biosensors and Bioelectronics 2014, 56, 186–191. [PubMed: 24487255]
28. Lyandres O; Shah NC; Yonzon CR; Walsh JT; Glucksberg MR; Van Duyne RP, Real-Time Glucose Sensing by Surface-Enhanced Raman Spectroscopy in Bovine Plasma Facilitated by a Mixed Decanethiol/Mercaptohexanol Partition Layer. Analytical Chemistry 2005, 77 (19), 6134–6139. [PubMed: 16194070]
29. Sharma B; Bugga P; Madison LR; Henry A-I; Blaber MG; Greeneltch NG; Chiang N; Mrksich M; Schatz GC; Van Duyne RP, Bisboronic Acids for Selective, Physiologically Relevant Direct Glucose Sensing with Surface-Enhanced Raman Spectroscopy. Journal of the American Chemical Society 2016, 138 (42), 13952–13959.
30. Negri P; Sarver SA; Schiavone NM; Dovichi NJ; Schultz ZD, Online SERS detection and characterization of eight biologically-active peptides separated by capillary zone electrophoresis. Analyst 2015, 140 (5), 1516–22. [PubMed: 25599104]
31. Wishart DS; Feunang YD; Marcu A; Guo AC; Liang K; Vazquez-Fresno R; Sajed T; Johnson D; Li C; Karu N; Sayeeda Z; Lo E; Assempour N; Berjanskii M; Singhal S; Arndt D; Liang Y; Badran H; Grant J; Serra-Cayuela A; Liu Y; Mandal R; Neveu V; Pon A; Knox C; Wilson M; Manach C;

Scalbert A, HMDB 4.0: the human metabolome database for 2018. Nucleic Acids Res 2018, 46 (D1), D608–D617. [PubMed: 29140435]

32. Riordan CM; Jacobs KT; Negri P; Schultz ZD, Sheath flow SERS for chemical profiling in urine. Faraday Discussions 2016, 187 (0), 473–484. [PubMed: 27034996]
33. Camden JP; Dieringer JA; Zhao J; Van Duyne RP, Controlled Plasmonic Nanostructures for Surface-Enhanced Spectroscopy and Sensing. Accounts of Chemical Research 2008, 41 (12), 1653–1661. [PubMed: 18630932]
34. Stiles PL; Dieringer JA; Shah NC; Van Duyne RP, Surface-enhanced Raman spectroscopy. Annu Rev Anal Chem (Palo Alto Calif) 2008, 1, 601–26. [PubMed: 20636091]
35. Alam R; Lightcap IV; Karwacki CJ; Kamat PV, Sense and shoot: simultaneous detection and degradation of low-level contaminants using graphene-based smart material assembly. ACS Nano 2014, 8 (7), 7272–8. [PubMed: 24893206]
36. Matulaitienė I; Kuodis Z; Matijoška A; Eicher-Lorka O; Niaura G, SERS of the Positive Charge Bearing Pyridinium Ring Terminated Self-Assembled Monolayers: Structure and Bonding Spectral Markers. The Journal of Physical Chemistry C 2015, 119 (47), 26481–26492.
37. Palazon F; Benavides CM; Leonard D; Souteyrand E; Chevolot Y; Cloarec JP, Carbodiimide/NHS derivatization of COOH-terminated SAMs: activation or byproduct formation? Langmuir 2014, 30 (16), 4545–50. [PubMed: 24720739]
38. Subaihi A; Trivedi DK; Hollywood KA; Bluett J; Xu Y; Muhamadali H; Ellis DI; Goodacre R, Quantitative Online Liquid Chromatography-Surface-Enhanced Raman Scattering (LC-SERS) of Methotrexate and its Major Metabolites. Anal Chem 2017, 89 (12), 6702–6709. [PubMed: 28505414]
39. Zaffino C; Bedini Giulia D; Mazzola G; Guglielmi V; Bruni S, Online coupling of high-performance liquid chromatography with surface-enhanced Raman spectroscopy for the identification of historical dyes. Journal of Raman Spectroscopy 2016, 47 (5), 607–615.
40. Cabalin LM; Ruperez A; Laserna JJ, Surfaceenhanced Raman spectrometry for detection in liquid chromatography using a windowless flow cell. Talanta 1993, 40 (11), 1741–1747. [PubMed: 18965847]
41. Guerrini L; Krpetic Z; van Lierop D; Alvarez-Puebla RA; Graham D, Direct surface-enhanced Raman scattering analysis of DNA duplexes. Angew Chem Int Ed Engl 2015, 54 (4), 1144–8. [PubMed: 25414148]
42. Ratkaj M; Biljan T; Miljanić S, Quantitative Analysis of Entacapone Isomers Using Surface-Enhanced Raman Spectroscopy and Partial Least Squares Regression. Applied Spectroscopy 2012, 66 (12), 1468–1474. [PubMed: 23231910]

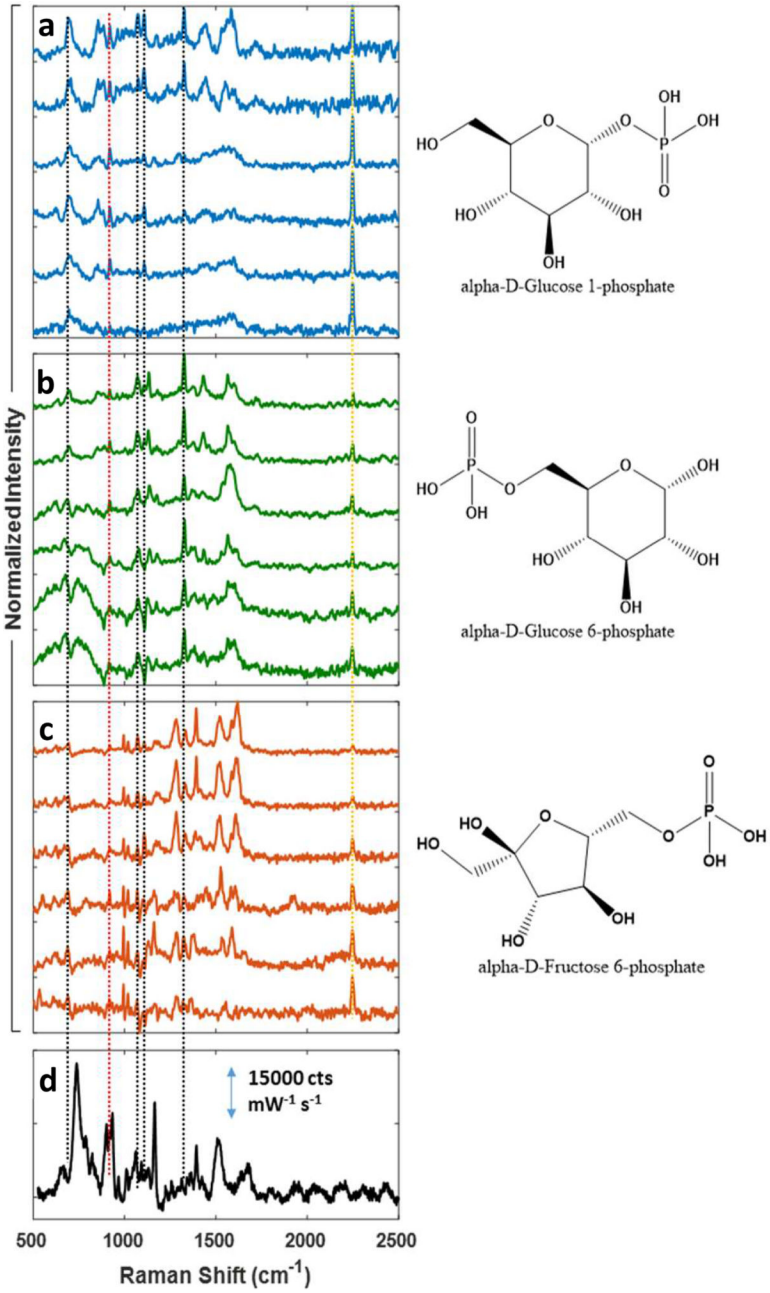

Figure 1.

SERS spectra obtained at different analyte concentration are shown for: (a) G1P (top-bottom: 20 μM, 10 μM, 4 μM, 1 μM, 0.5 μM, and 0.25 μM) (b) G6P (top-bottom: 20 μM, 10 μM, 4 μM, 1 μM, 0.5 μM, and 0.25 μM), (c) F6P (top-bottom: 20 μM, 8 μM, 4 μM, 2 μM, 1 μM, and 0.5 μM). The SERS spectrum of the hexanethiol SAM on silver substrate is shown in (d). The spectra in (a), (b), and (c) were background subtracted using the monolayer spectrum (d) and row normalized. The phosphate group stretching is observed at 921 cm^{-1} (red dotted line). The black dotted lines indicate common peaks between the three analytes that correspond to previously reported SERS signals of glucose. The acetonitrile signal, which was used as an internal standard, was observed at 2250 cm^{-1} (yellow dotted line).

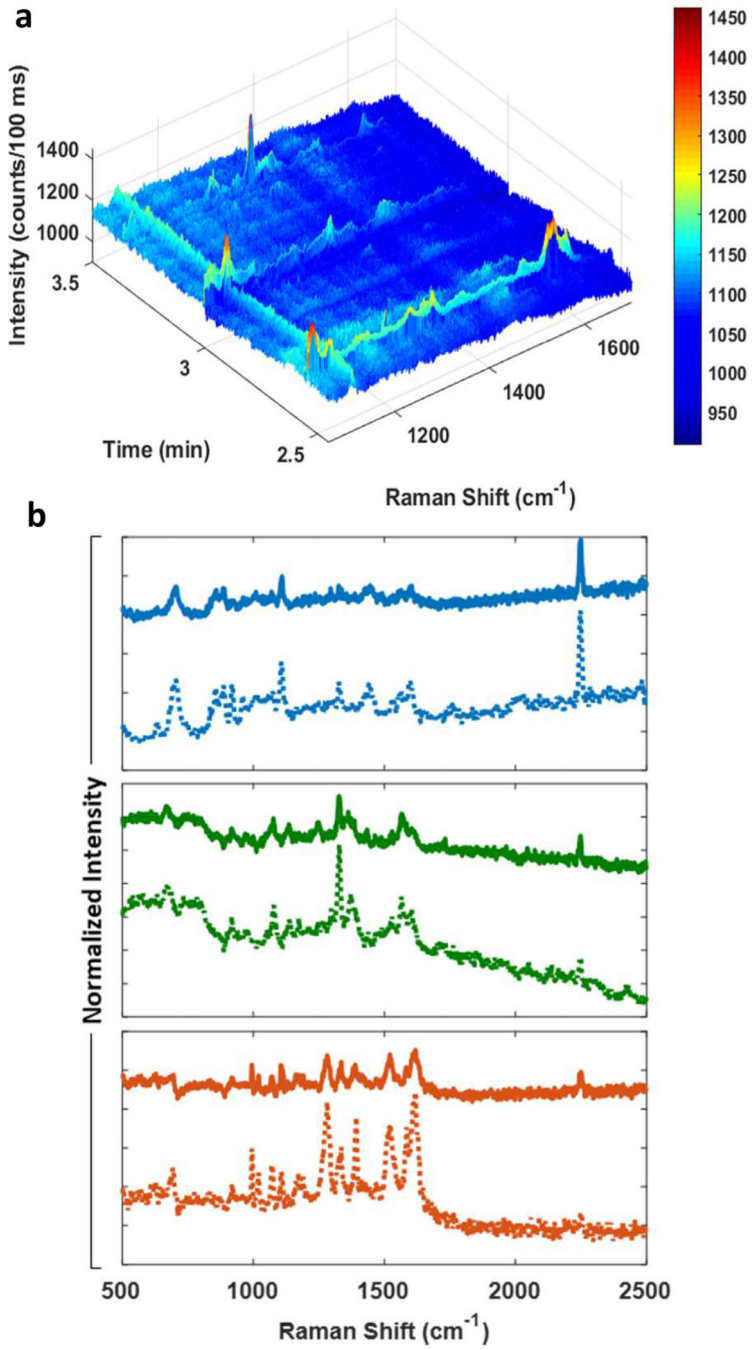

Figure 2.

(a) The SERS chromatogram obtained from a mixture of 2 μM of the three analytes in water is shown. The retention times are 2.6 ± 0.3 mins, 3.0 ± 0.3 mins, and 3.5 ± 0.2 mins for F6P, G1P and G6P, respectively. (b) The extracted SERS spectrum of G1P (blue top spectrum), G6P (green top spectrum), and F6P (orange top spectrum) were compared to their reference spectra obtained from direct injection (bottom spectra, dotted).

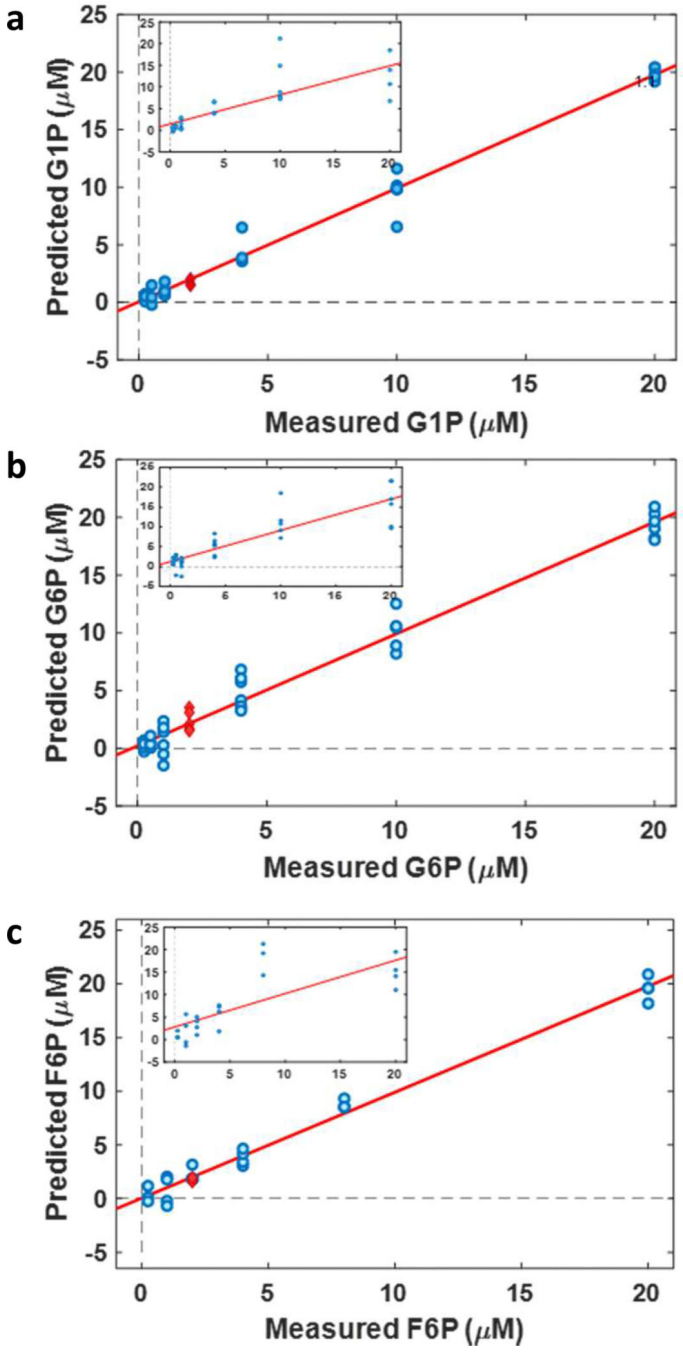

Figure 3.

PLS regression models for (a) G1P, (b) G6P, and (c) F6P show the predicted concentrations versus known concentrations. The concentration-dependent spectra of each analyte was normalized against the intensity of the acetonitrile internal standard. Red data points represent the SERS measurements in pure mixture containing 2μM of each analyte being projected along the fit line of the PLS model. The inset plots PLS calibration model built without the internal standard and show a non-linear dependence.

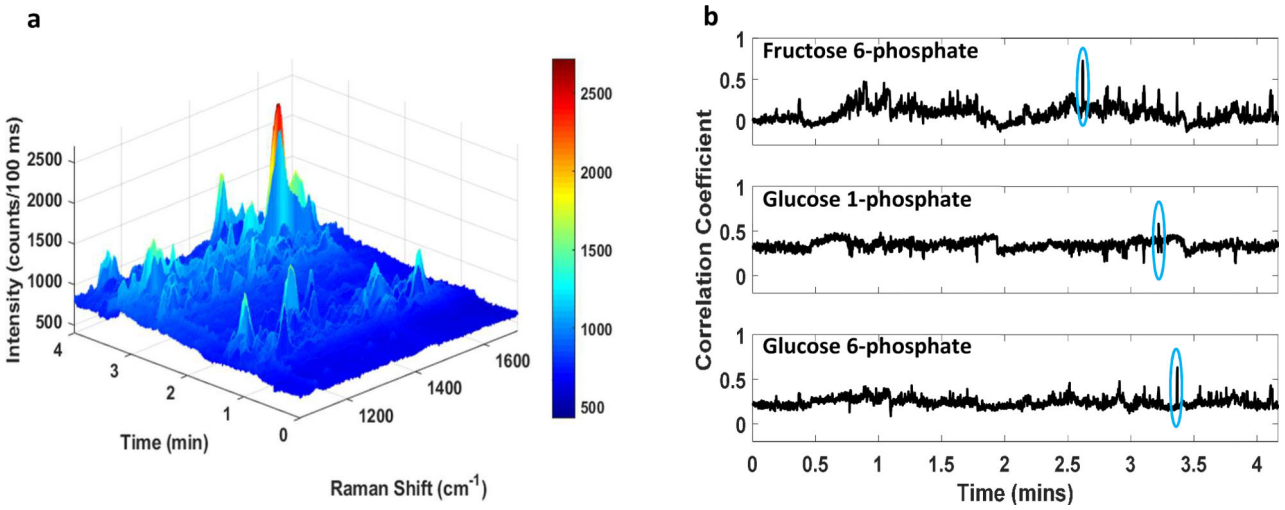

Figure 4.

(a) LC-SERS chromatogram of G1P, G6P and F6P mixture spiked into cell culture media to provide a sample concentration of 2 μM for each analyte shows several closely eluting molecules. (b) The Pearson correlation coefficient plots show the correlation between every spectrum in the LC-SERS chromatogram against the reference spectra of each analyte. The highlighted regions illustrate the observed highest correlation for each analyte in the chromatogram

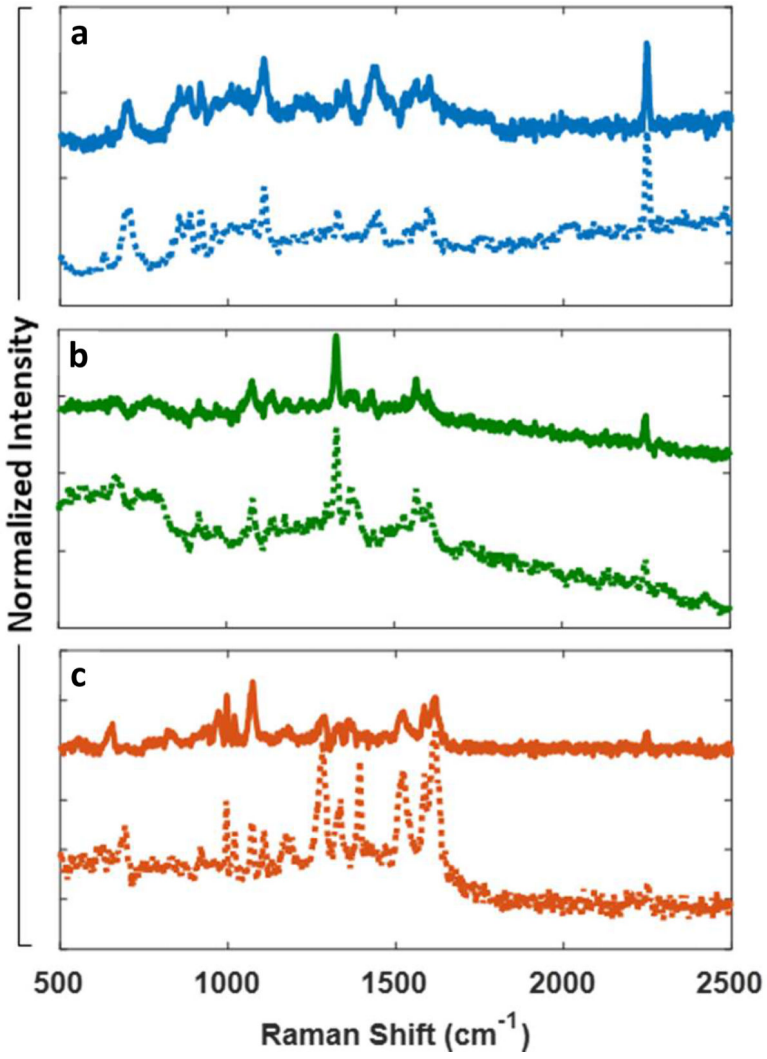

Figure 5.

The SERS spectra (solid line) at the highest correlation time points from Figure 4 were extracted and compared with reference spectra (dotted line) to confirm the identification of (a) G1P, (b) G6P, and (c) F6P.

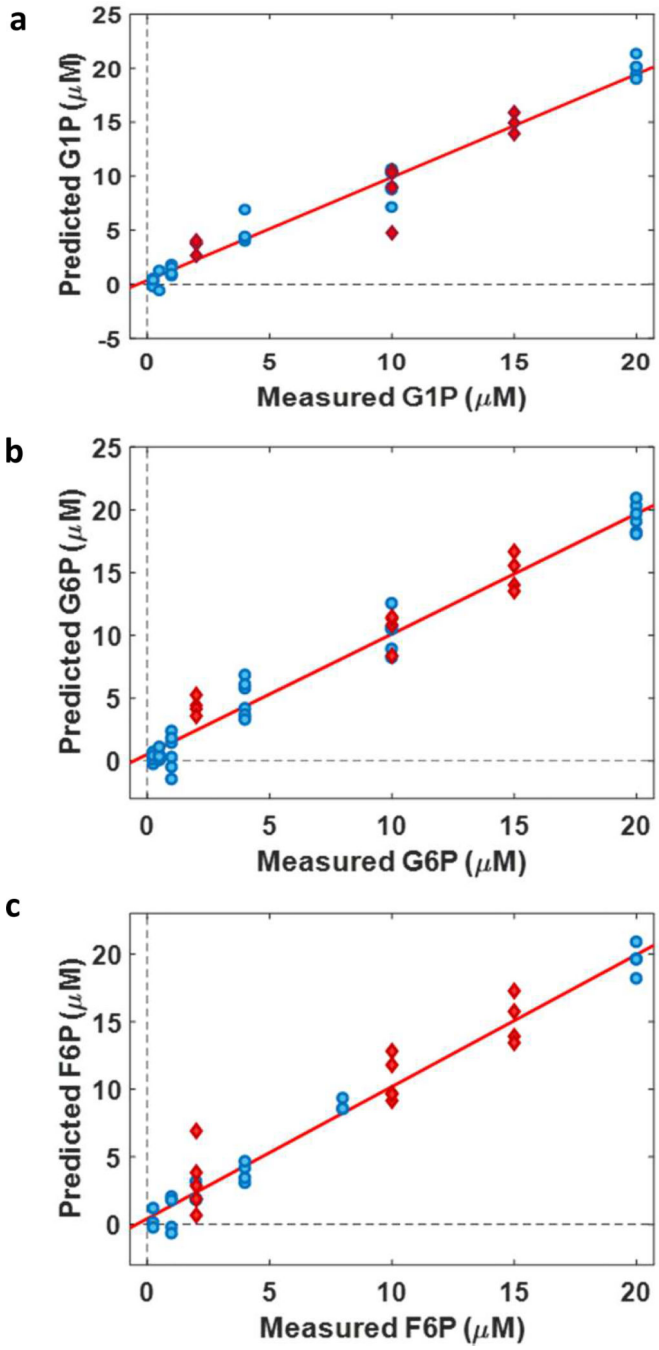

Figure 6.

The SERS spectra from the analytes: (a) G1P, (b) G6P, and (c) F6P, spiked in cell culture media were validated using a PLS model from pure components (Figure 3) to identify their concentrations. The test data point (red) project well along the best fit line.